

1 **Discovery and Multi-center Verification of Prostate Cancer Protein Biomarkers using Single-**
2 **shot Short Gradient Microflow SWATH and MRM^{HR} Mass Spectrometry**

3 Rui Sun 1,2*, Christie Hunter 3*#, Chen Chen 4, Weigang Ge 1,2, Nick Morrice 3, Qiushi Zhang 1,2,
4 Xue Cai 1,2, Bo Wang 5, Xiaoyan Yu 6, Xiaodong Teng 5, Lirong Chen 6, Shaozheng Dai 7, Jian
5 Song 8, Zhongzhi Luan 7, Changbin Yu 8, Ruedi Aebersold 9, Yi Zhu 1,2#, Tiannan Guo 1,2 #

6

7 1, Key Laboratory of Structural Biology of Zhejiang Province, School of Life Sciences, Westlake
8 University, 18 Shilongshan Road, Hangzhou 310024, Zhejiang Province, China

9 2, Institute of Basic Medical Sciences, Westlake Institute for Advanced Study, 18 Shilongshan Road,
10 Hangzhou 310024, Zhejiang Province, China

11 3, SCIEX, USA

12 4, SCIEX, China

13 5, Department of Pathology, The First Affiliated Hospital of College of Medicine, Zhejiang
14 University, Hangzhou, China

15 6, Department of Pathology, The Second Affiliated Hospital, Zhejiang University School of Medicine,
16 Hangzhou, Zhejiang, 310009, China

17 7, School of Computer Science and Engineering, Beihang University, Beijing, China

18 8, School of Engineering, Westlake University, 18 Shilongshan Road, Hangzhou 310024, Zhejiang
19 Province, China

20 9, Department of Biology, Institute of Molecular Systems Biology, ETH Zurich, Switzerland

21

22 * co-first

23 # co-correspondence

24 **Emails:**

25 Rui Sun: sunrui@westlake.edu.cn 0000-0002-8484-8089

26 Christie Hunter: Christie.Hunter@sciex.com 0000-0003-2587-1489

27 Chen Chen: chen.chen@sciex.com

28 Weigang Ge: geweigang@westlake.edu.cn 0000-0002-1803-4327

29 Nick Morrice: nick.morrice@sciex.com

30 Qiushi Zhang: zhangqiushi@westlake.edu.cn 0000-0001-5169-2092

31 Xue Cai: caixue@westlake.edu.cn 0000-0002-7427-2100

32 Bo Wang: 1506128@zju.edu.cn

33 Xiaoyan Yu: greg.sander15@yahoo.com

34 Xiaodong Teng: 1102069@zju.edu.cn

35 Lirong Chen: chenlr999@163.com

36 Shaozhi Dai: daiszemail@126.com 0000-0001-8901-1272

37 Jian Song: songjian@westlake.edu.cn

38 Zhongzhi Luan: luan.zhongzhi@buaa.edu.cn 0000-0002-7186-0556

39 Changbin Yu: yu_lab@westlake.edu.cn

40 Ruedi Aebersold: aebersold@imsb.biol.ethz.ch

41 Yi Zhu: zhuyi@westlake.edu.cn 0000-0003-0429-0802

42 Tiannan Guo: guotiannan@westlake.edu.cn 0000-0003-3869-7651

43

44 **Abstract (limit 250 words)**

45 **BACKGROUND:** Discovery and verification of protein biomarkers in clinical specimens using mass
46 spectrometry are inherently challenging and resource-intensive.

47 **METHODS:** Formalin-fixed paraffin-embedded tissue-biopsy samples from a prostate cancer patient
48 cohort (PCZA, n = 68) were processed in triplicate using pressure cycling technology, followed by
49 microflow LC SWATH[®] analysis with different gradients and window schemes. Potential protein
50 biomarker candidates were prioritized using random forest analysis and evaluated by receiver
51 operating characteristic curve analysis. Selected proteins were verified with a targeted MRM^{HR} assay
52 using the 15 min microflow LC strategy on a second prostate cancer cohort (PCZB, n = 54). Potential
53 biomarkers were further verified using TMA on a third cohort (PCZD, n = 100).

54 **RESULTS:** We developed and optimized a 15-min microflow LC approach coupled with microflow
55 SWATH MS. Application of the optimal 15 min and conventional 120 min LC gradient scheme using
56 samples from the PCZA cohort led to quantification of 3,800 proteins in both methods with high
57 quantitative correlation ($r = 0.77$). MRM^{HR} verification of 154 prioritized proteins showed high
58 quantitative consistency with the 15 min SWATH data ($r = 0.89$). Separation of benign and malignant
59 tissues achieved precision (AUC = 0.99). ECHS1 was further verified in a third cohort PCZD
60 successfully, agreeing with RNAseq data from the TCGA in a different cohort (n=549). Our methods
61 enables practical proteomic analysis of 204 tissue samples within 5 working days.

62 **CONCLUSION:** Single-shot, short gradient SWATH-MS coupled with MRM^{HR} is both practical and
63 effective in discovering and verifying protein biomarkers in clinical specimens.

64

65 **Introduction**

66 Prostate cancer (PCa) is a group of complex diseases that occur in the prostate gland, resulting
67 from carcinogenesis that leads to the modulation of a number of proteins. The regulated proteins in
68 malignant prostate tissue samples reflect the molecular pathology of these complex diseases and offer
69 a plethora of drug targets[1]. Due to the high degree of inter-patient and inter-tissue heterogeneity, it is
70 crucial to identify differentially expressed proteins in prostate cancer cohorts and verify them in multi-
71 center studies. However, this is inherently challenging and resource-intensive mainly due to the lack
72 of high-throughput protein biomarker discovery and verification methods.

73 Typically, proteomes are analyzed using shotgun proteomics by multi-dimensional fractionation
74 based on the need to isolate each peptide precursor for fragmentation, sequencing, and quantification.
75 Isotopic labeling technologies including SILAC, iTRAQ, and TMT increase the multiplexing
76 capability of shotgun proteomics; however, they remain resource-intensive for analyzing clinical
77 cohorts. Several proteomics studies using these methods have reportedly analyzed up to 200 clinical
78 samples [2]; however, very few laboratories—even well-equipped ones—can carry out such
79 expensive investigations. Many researchers have been striving to shorten the LC gradient time to
80 increase the efficiency of shotgun proteomics analysis. For example, by integrating multiple pre-
81 fractionations with relatively shorter LC gradients, in-depth MS analysis of a whole proteome can be
82 achieved [3]. However, this analytical approach lacks reproducibility and is time consuming, posing a
83 challenge in applying it to quantitative clinical studies for biomarker discovery for which hundreds to
84 thousands of patients are usually recruited. A faster method based on Nano-LC and Orbitrap MS has
85 been reported recently [4] that achieved high throughput, with 60 samples per working day with a 21-
86 min nano-LC system. However, the robustness and reproducibility of this method for large numbers
87 of tissue samples in cohort studies remain to be evaluated.

88 SWATH/DIA mass spectrometry [5], which identifies and quantifies peptide precursors via
89 chromatographic peak groups from highly convoluted mass spectra [6], bypasses the need to isolate
90 peptide precursors during acquisition, improving data completeness and enabling efficient single-shot
91 proteomic analysis. The key to this MS technique is the ability to collect high resolution MS/MS
92 spectra at very high acquisition rates, such that a wide mass range can be covered with a series of

93 smaller Q1 isolation windows in an LC-compatible cycle time. Thus, the rapid scanning rate of
94 TripleTOF® systems has been the key to enabling the shortening of LC gradients for analyzing
95 complex tissue proteomes, from 120 min [6] to 45 min [7], without compromising proteome depth;
96 this method is increasingly applied to analyze various types of clinical samples including plasma [8]
97 as well as tumor tissues [6, 7, 9].

98 An increasing number of studies have demonstrated the applicability of microflow
99 chromatography coupled with SWATH-MS [10-14], especially with regard to clinical applications. In
100 this study, we combined microflow LC with SWATH-MS to perform a quantitative proteomics study
101 of PCa tissue-biopsies in a high throughput manner by further shortening the LC gradient—a method
102 referred to as single-shot short gradient microflow SWATH acquisition (S3 SWATH MS). After
103 benchmarking, we applied S3 SWATH to discover protein biomarker candidates from a prostate
104 cancer cohort, some of which were further validated orthogonally using independent cohorts and
105 MRM^{HR} verification.

106

107 **Materials and Methods**

108 **Standard protein digests**

109 HEK 293 cell digests were prepared as has been previously described [15] and were provided by
110 Dr Yansheng Liu. K562 cell digests were obtained from the SWATH Performance Kit (SCIEX,
111 Framingham, MA, USA). iRT peptides (Biognosys, Schlieren, Switzerland) were spiked into peptide
112 samples at a final concentration of 10% prior to MS analysis for retention time (RT) calibration.

113 **PCa patient cohorts and formalin-fixed paraffin-embedded (FFPE) samples**

114 The PCZA and PCZB cohorts were acquired from the Second Affiliated Hospital College of
115 Medicine, Zhejiang University. The PCZD cohort was collected from the First Affiliated Hospital
116 College of Medicine, Zhejiang University. All patients were recruited from 2017 to 2018. All cohorts
117 were approved by the ethics committee of their respective hospitals.

118 The PCZA cohort was composed of 58 PCa patients and 10 benign prostatic hyperplasia (BPH)
119 patients. The PCZB cohort included 24 PCa patients and 30 BPH patients, while the PCZD cohort
120 contained 70 PCa patients and 30 BPH patients.

121 In the PCZA cohort, three biological replicates (size $1 \times 1 \times 5 \text{ mm}^3$) were collected and analyzed
122 by SWATH MS and MRM^{HR}. In the PCZB cohort, two biological replicates ($1.5 \times 1.5 \times 5 \text{ mm}^3$) were
123 analyzed by MRM^{HR}. In the PCZD cohort, one punch ($1.5 \times 1.5 \times 5 \text{ mm}^3$) was used for each sample
124 for TMA validation.

125 **Pressure cycling technology (PCT)-assisted peptide extraction from FFPE tissues**

126 Approximately 0.5 mg of an FFPE tissue punch was weighed and processed for each biological
127 replicate via the FFPE-PCT workflow as described previously [16]. Briefly, the tissue punches were
128 first dewaxed by incubating with 1 mL of heptane under gentle vortexing at 600–800 rpm, followed
129 by serial rehydration using 1 mL of 100%, 90%, and 75% ethanol, respectively. Tissues were further
130 incubated with 200 μL of 0.1% formic acid (FA) at 30 °C for 30 min for acidic hydrolysis. The tissue
131 punches were then transferred into PCT-MicroTubes and were briefly washed with 100 μL of fresh
132 0.1 M Tris-HCl (pH 10.0) to remove FA residues. Thereafter, the tissues were incubated with 15 μL of
133 freshly prepared 0.1 M Tris-HCl (pH 10.0) at 95 °C for 30 min with gentle vortexing at 600 rpm.
134 Samples were immediately cooled to 4 °C after basic hydrolysis.

135 Following the pretreatment described above, 25 μL of lysis buffer (6 M urea, 2 M thiourea, 5
136 mM Na₂EDTA in 100 mM ammonium bicarbonate, pH 8.5) was added to the PCT-MicroTubes
137 containing tissues and protein extracts that were soaked previously in 15 μL of 0.1 M Tris-HCl (pH
138 10.0). The tissue samples were further subjected to PCT-assisted tissue lysis and protein digestion
139 procedures using the Barocycler NEP2320-45K (Pressure Biosciences Inc., Boston, MA, USA) as

140 described previously [17]. The PCT scheme for tissue lysis was set such that each cycle involved 30 s
141 of high pressure at 45 kpsi and 10 s of ambient pressure, oscillating for 90 cycles at 30 °C. Protein
142 reduction and alkylation was performed at ambient pressure by incubating protein extracts with 10
143 mM Tris(2-carboxyethyl) phosphine (TCEP) and 20 mM iodoacetamide (IAA) in darkness at 25 °C
144 for 30 min, with gentle vortexing at 600 rpm in a thermomixer. Then the proteins were digested with
145 MS grade Lys-C (enzyme-to-substrate ratio, 1:40) using a PCT scheme set to 50 s of high pressure at
146 20 kpsi and 10 s of ambient pressure for each cycle, oscillating for 45 cycles at 30 °C. Thereafter, the
147 proteins were further digested with MS grade trypsin (enzyme-to-substrate ratio, 1:50) using a PCT
148 scheme with 50 s of high pressure at 20 kpsi and 10 s of ambient pressure in one cycle, oscillating for
149 90 cycles at 30 °C. Peptide digests were then acidified with 1% trifluoroacetic (TFA) to pH 2–3 and
150 subjected to C18 desalting. iRT peptides were spiked into peptide samples at a final concentration of
151 10% prior to MS analysis for RT calibration.

152 **Optimization of microflow LC gradients coupled with SWATH MS**

153 During the optimization studies, peptide samples were separated with different microflow
154 gradients and different SWATH-MS parameters. Linear gradients of 3–35% acetonitrile (0.1% formic
155 acid) with durations of 5, 10, 20, 30, and 45 min were evaluated. The number of Q1 variable windows
156 (40, 60, 100) and MS/MS accumulation time (15, 25 ms) constituted the key parameters that were
157 adjusted for the shorter gradients. The need for collision energy spread with the optimized collision
158 energy ramps was tested. Four replicates were performed for each test, after which the data were
159 processed with PeakView® software with the SWATH 2.0 MicroApp to evaluate the number of
160 proteins and peptides quantified at <1 % FDR and with < 20% CV. The optimized methods were then
161 tested on multiple instruments with different cell lysates to confirm the robustness of the observations.

162 **S3 SWATH MS acquisition**

163 Peptides were separated at a flow rate of 5 µL/min along a 15 min 5–35% linear LC gradient
164 (buffer A: 2% ACN, 0.1% formic acid; buffer B: 80% ACN, 0.1% formic acid) using an Eksigent
165 NanoLC 400 System coupled to a TripleTOF® 6600 system (SCIEX). The DuoSpray Source was
166 replumbed using 25 µm ID hybrid electrodes to minimize post-column dead volume. The SWATH
167 method consisted of a 150 ms TOF MS scan with m/z ranging from 350 to 1250 Da, followed by
168 MS/MS scans performed on all precursors (from 100 to 1500 Da) in a cyclic manner. A 100 variable
169 Q1 isolation window scheme was used in this study (Supplemental Table 1B). The accumulation time
170 was set at 25 ms per isolation window, resulting in a total cycle time of 2.7 s.

171 For the beta-galactosidase digest (β-gal) calibration analysis, peptides were separated at a
172 flowrate of 5 µL/min along a 5 min 5–35% linear LC gradient (buffer A: 2% ACN, 0.1% formic acid;
173 buffer B: 80% ACN, 0.1% formic acid) using an Eksigent NanoLC 400 System coupled to a
174 TripleTOF® 6600 system (SCIEX). The DuoSpray Source was replumbed using 25 µm ID hybrid
175 electrodes to minimize post-column dead volume. The MS method consisted of a 250 ms TOF MS
176 scan with m/z ranging from 400 to 1250 Da, followed by a 500 ms product ion scan (target m/z =
177 729.4, indicating a peptide in the β-gal digest mixture) with a scan range of 100–1500, high sensitivity
178 mode. The RT, intensity, and m/z of targeted precursor and fragment ions were used for LC QC, the
179 sensitivity test, and mass calibration separately.

180 **MRM^{HR} MS acquisition**

181 A time scheduled MRM^{HR} targeted quantification strategy was used to further validate proteins
182 observed to be differentially expressed based on the SWATH quantification described above. Peptides
183 were separated at 5 µL/min using the same microflow LC approach as that used for S3 SWATH MS
184 analysis. The TripleTOF® 6600 mass spectrometer was operated in IDA mode for time-scheduling the
185 MS/MS acquisition for 286 peptides for the MRM^{HR} workflow. The method consisted of one 75 ms
186 TOF-MS scan for precursor ions with m/z ranging from 350 to 1250 Da, followed by MS/MS scans
187 for fragment ions with m/z ranging from 100 to 1500 Da, allowing for a maximum of 45 candidate
188 ions to monitor per cycle (25 ms accumulation time, 50 ppm mass tolerance, rolling collision energy,
189 +2 to +5 charge states with intensity criteria above 2 000 000 cps to guarantee that no untargeted

190 peptides would be acquired). The fragment information including m/z and RT of a targeted precursor
191 ion was confirmed by previous SWATH results and was then added to the inclusion list for the
192 targeted analysis. The intensity threshold of targeted precursors in the inclusion list was set to 0 cps
193 and the scheduling window was 60 s. The targeted peptide sequences were the same as those found in
194 the previous SWATH MS analysis.

195 Targeted MRM^{HR} data were analyzed by Skyline [18], which automatically detected the
196 extracted-ion chromatogram (XIC) from an LC run by matching the MS spectra of the targeted ion
197 against its spectral library generated from the IDA mode within a specific mass tolerance window
198 around its m/z. All peaks selected were checked manually after automated peak detection using
199 Skyline. Both MS1 and MS2 filtering were set as “TOF mass analyzer” with a resolution power of 30
200 000 and 15 000, respectively, while the “Targeted” acquisition method was defined in the MS/MS
201 filtering.

202 **SWATH data analysis**

203 The optimization data for optimal LC gradients were processed using the SWATH 2.0 MicroApp
204 in PeakView® software (SCIEX) using the Pan Human Library [19]. RT calibration was performed
205 first using iRT peptides for an adjusted RT window at a 75 ppm XIC extraction width. Replicate
206 analysis was performed using the SWATH Replicate Analysis Template (SCIEX) to determine the
207 number of peptides and proteins quantified at a 1% peptide FDR and < 10 or 20% CV.

208 The prostate samples were processed using the OpenSWATH pipeline. Briefly, SWATH raw data
209 files were converted in profile mode to mzXML using msconvert and analyzed using OpenSWATH
210 (2.0.0) [5] as described previously [6]. The RT extraction window was 600 s and m/z extraction was
211 performed with 0.03 Da tolerance. RT was then calibrated using both iRT peptides. Peptide precursors
212 were identified by OpenSWATH and PyProphet with d_score > 0.01. For each protein, the median
213 MS2 intensity value of peptide precursor fragments, which were detected to belong to the protein was
214 used to represent the protein abundance.

215 **Tissue microarray analysis**

216 The TMA and IHC procedures used in this study have been described previously [20]. The ESCH
217 antibody was acquired from Proteintech (66489-1-Ig; Chicago, IL, USA).

218

219 **Results and Discussion**

220 **Establishment of the S3 SWATH MS method**

221 We first optimized the short microflow LC gradient using the TripleTOF® 6600 system. A series
222 of LC gradient lengths ranging from 5, 10, 20, and 45 min were tested (**Table S1**). For each LC
223 condition, the number of variable Q1 windows (60 and 100) were investigated. More acquisition
224 windows require shorter MS/MS accumulation times to maintain an LC compatible cycle time;
225 therefore, two different MS/MS accumulation times, 15 and 25 ms, were tested (**Fig. 1a**). These
226 adjustments were aimed to ensure reasonable data points across the narrower chromatography peaks
227 that are obtained with faster LC gradients.

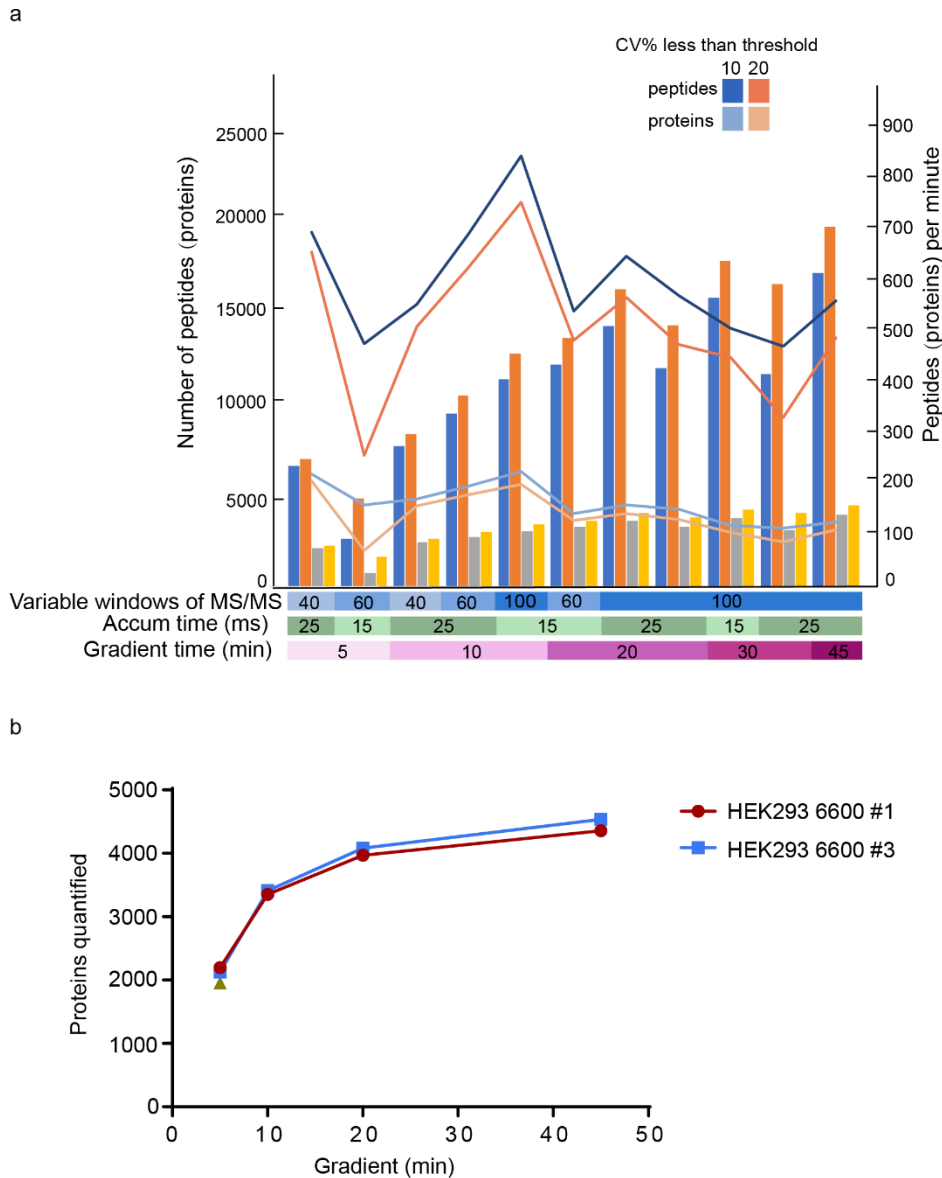
228 Standard HEK 293 cell lysate digests were used for the optimization. One microgram of peptides
229 was loaded onto the microflow column. For each optimization condition, four technical replicates
230 were analyzed. The data were processed and evaluated according to the number of proteins and
231 peptides quantified with FDR < 1% and CV < 10% or CV < 20%, respectively. The data acquired with
232 20 min microflow LC gradient enabled the quantification of 90% of the proteins as quantified by the
233 45 min microflow LC gradient method (**Fig. 1a**). Using the optimized 20 min gradient method, we
234 identified 14,112 peptides and 3523 proteins with CV below 10% when the Q1 window was fixed at
235 100. Decreasing the MS/MS accumulation time to 15 ms was tested and did contribute to higher
236 numbers of protein and peptide identifications, especially for the 5 and 10 min LC gradients.
237 Calculation of the number of peptides identified per time unit (min) further showed that the LC-MS

238 condition involving a 10 min microflow LC gradient plus 100 Q1 windows with the MS/MS
239 accumulation time of 15 ms resulted in the highest number of identified peptides per time unit.
240 Typically, using more variable Q1 isolation windows provided improved quantitative results most
241 likely because of reduced signal/noise due to increased coelution of peptides. The MS/MS
242 accumulation time was shortened to account for the much narrower LC peak widths.

243 After the optimization experiments, the best condition for each gradient length with optimal
244 windows and MS/MS accumulation time was used to analyze the HEK293 cell line proteome on
245 multiple instruments to fully characterize the impact of gradient length on SWATH quantitation (**Fig.**
246 **1b**). As expected, as the gradients were shortened, fewer proteins and peptides could be reliably
247 quantified. The 20 min gradient using the best acquisition conditions quantified ~91% and ~83% of
248 the proteins and peptides, respectively, that were quantified during the 45 min gradient with a 1 µg
249 peptide load. The 10 min gradient using the best acquisition conditions quantified ~77% and ~65 % of
250 the proteins and peptides, respectively, that were quantified during the 45 min gradient with a 1 µg
251 peptide load. A total of 3354 proteins were reproducibly quantified at < 20% CV using the 10 min
252 gradient (**Fig. 1b**). That said, the reduction in quantified proteins was less than expected when
253 compared to the 45 min gradient with a 1 µg peptide load. These results confirmed that accelerated
254 microflow SWATH experiments, i.e., the S3 SWATH method, can be applied to biomarker research
255 studies where large cohorts are available and high throughput is desired.

256

257



258

259 **Figure 1. Optimization of S3 SWATH acquisition using HEK 293 cell lysate. (a)** Using a series of
 260 microflow LC gradient lengths, the SWATH acquisition conditions were optimized to determine the
 261 best acquisition and processing settings for the accelerated analysis. The number of proteins and
 262 peptides were quantified with the cutoff of FDR < 1% and CV < 10% or < 20% calculated from four
 263 technical replicates for each tested condition. **(b)** Using the optimized conditions determined for each
 264 gradient, several datasets were collected on two 6600 instruments to benchmark the impact on proteins
 265 quantified. The 10 and 20 min gradients allowed for ~70% and ~90%, respectively, of the proteins to
 266 be quantified as compared to the 45 min gradient.

267

268 To confirm the utility of S3 SWATH in a PCa patient cohort, we further tested the S3
 269 SWATH method using a PCa tissue pool which included three PCa and three BPH patient
 270 samples. We investigated the best MS acquisition and processing settings with each LC
 271 gradient of 10, 15, and 20 min gradients using a 1 µg peptide load in technical duplicate (**Fig.**
 272 **S1**). The 45 min microflow LC gradient with a 1 µg peptide load was used as reference. The
 273 15 min gradient was selected for use in the study, as there were 3263 proteotypic peptides and
 274 1367 SwissProt protein groups quantified with CV% below 10% for the 1 µg peptide load. As
 275 the use of shorter gradients is expected to have an effect on peak widths, S/N of data, etc., we
 276 also varied the RT extraction windows in the OpenSWATH analysis from 0 to 700 with a 10 s

277 interval and checked the protein identification (**Fig. S2**). Data showed that for both 10 min
278 and 20 min gradient S3-SWATH, the number of proteins identified saturated when the RT
279 extraction window was higher than 100 s.

280

281 **Application of S3 SWATH to a PCa patient cohort**

282 With the optimal S3 SWATH workflow, we analyzed the proteomes of the PCZA cohort
283 containing 58 PCa patient samples and 10 BPH patient samples. The demographic and
284 clinical information of these 68 patients are provided in **Table 1**; more details are available in
285 **Table S2**. Altogether, we processed 204 FFPE tissue punches (three biological replicates for
286 each sample) in seven batches (**Fig. 2a**), as well as quality control (QC) samples in each batch
287 for PCT-assisted digestion (**Fig. 2a**). These samples were analyzed with S3 SWATH on a
288 TripleTOF® 6600 mass spectrometer with QC runs for each MS batch. Automated β -gal
289 calibration and analytical column washing were performed every four sample injections
290 throughout the process (**Fig. 2b**). Taking into account the β -gal calibration, column washing
291 time, and control samples, the S3 SWATH method with 100 variable Q1 windows on the
292 TripleTOF® 6600 system completed the data acquisition for this cohort—in triplicates—in
293 125.7 hr (~5 days). We compared the S3 SWATH application in PCZA with another study by
294 our research group that involved use of the conventional SWATH method with 120 min LC
295 gradient and 48 variable Q1 windows in a TripleTOF® 5600+ [16]. The conventional method
296 required 467 hr (~20 days) to analyze the sample cohort (**Fig. 2b**). A total of 5059 and 4038
297 SwissProt proteins were quantified by the 120 and 15 min workflows, respectively, with a
298 quantitative reproducibility of CV < 20%. A total of 3800 proteins were found in common in
299 both data sets (**Fig. 2b**), comprising 75.1% of the proteins in the 120 min SWATH and 94.1%
300 proteins in the S3-SWATH. The S3 SWATH method gained a practical acceleration of 3.7
301 times when compared to the conventional method, with only a 24.88% loss of protein
302 identification.

303 Both methods achieved a high degree of quantitative reproducibility at the protein level
304 (**Fig. 2c**); the correlation coefficient between triplicates in the S3 SWATH method alone and
305 the 120 min SWATH MS method is 0.874 and 0.865, respectively, indicating the impressive
306 robustness of the S3 SWATH method. As for the 3800 proteins quantified, Pearson correlation
307 showed a high similarity ($r = 0.7681$) between the proteome data generated by the two
308 methods (**Fig. 2d**) and the correlation coefficient between two MS methods for individual
309 samples is over 0.7 (**Fig. S3**), further consolidating the high quantitative accuracy of the S3
310 SWATH method.

311

312 **Table 1. Demographic and clinical characteristics of the patients from different cohorts**

313

314

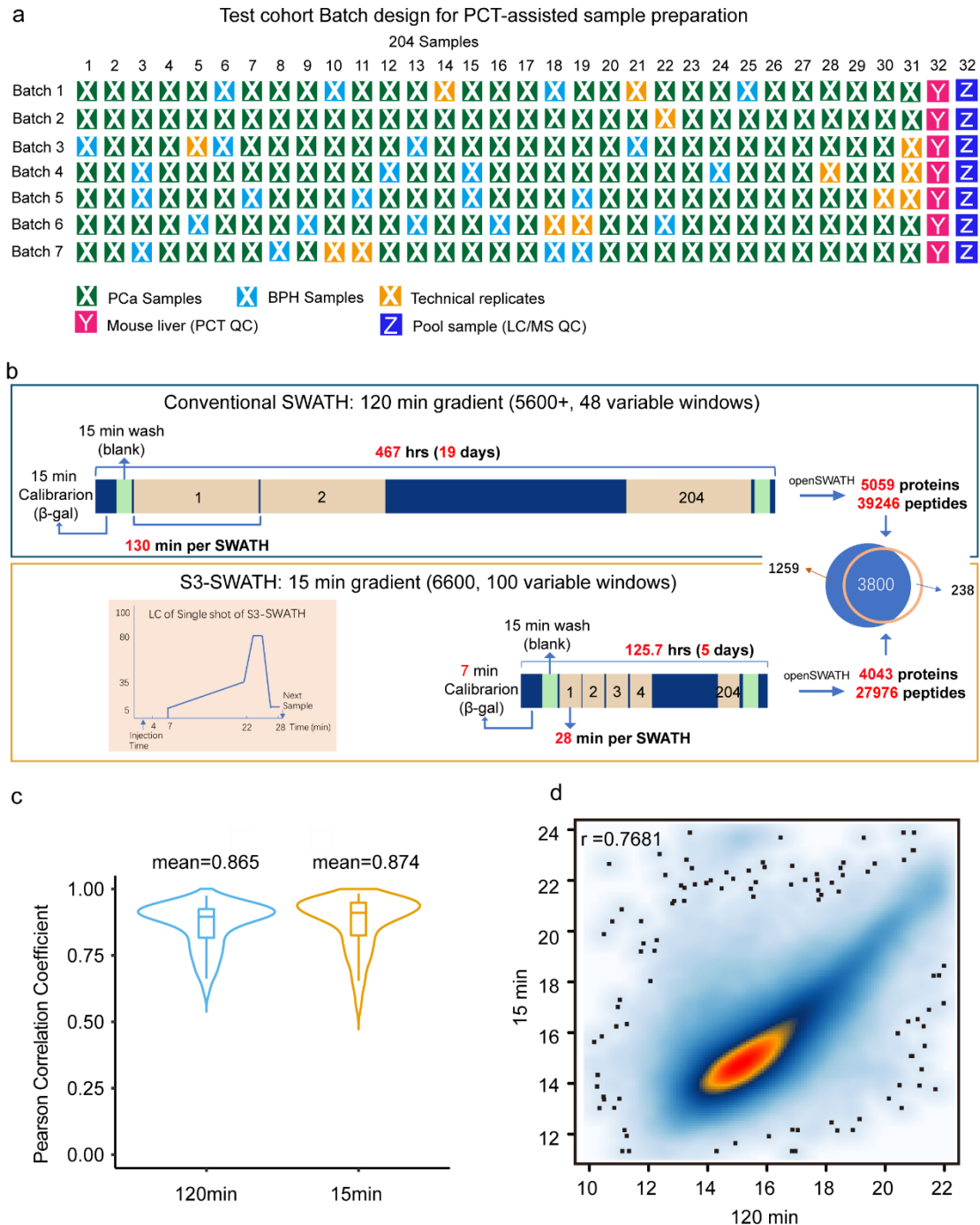
Cohorts	PCZA		PCZB		PCZD	
Tissue types	BPH=10	PCa=58	BPH=30	PCa=24	BPH=30	PCa=70
Biological replicates	n=3		n=2		n=1	
Age (yr)						
Median	68	67	69	70	70	67
Range	58-80	52-82	54-82	58-78	61-83	53-81
Gleason score						
Median	7		7		7	
Range	6-10		7-9		6-9	
3+3	0		0		0	
3+4	15		11		27	
4+3	19		8		30	
≥8	17		3		17	

315

316

317

318



319

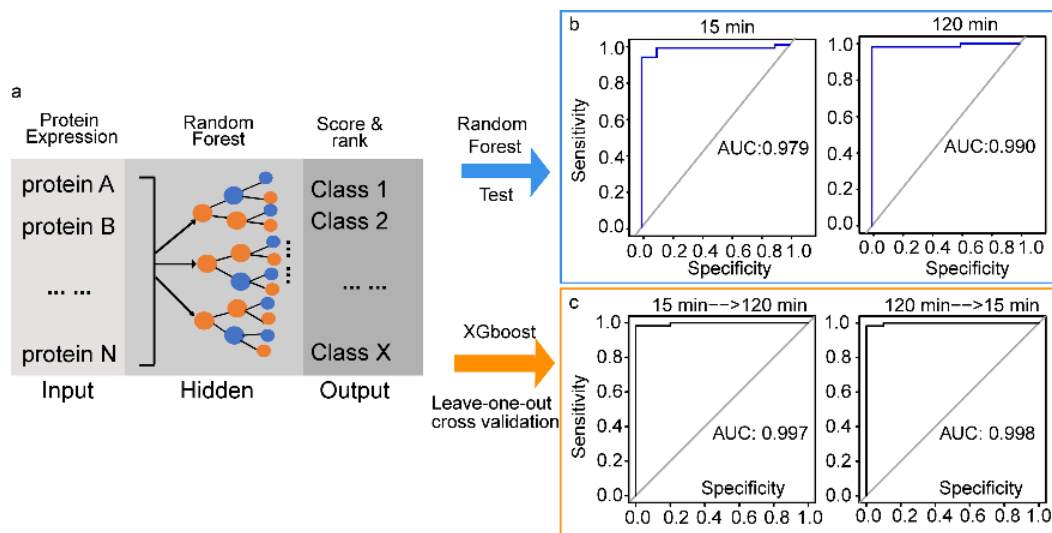
320 **Figure 2. Application of S3 SWATH to the PCZA cohort.** (a) Batch design of PCZA cohort. There
 321 are six batches of samples. Each batch contains PCa samples, BPH samples, technical replicates for
 322 randomly selected samples, mouse live-sample pool for PCT QC, and pooled prostate samples for LC-
 323 MS QC. (b) Workflow of the S3 SWATH and conventional SWATH. (c) Pearson correlation of 15 min
 324 and 120 min SWATH proteomes of the PCZA cohort. (d) Pearson correlation of 3800 proteins that
 325 were quantified by both 15 min and 120 min SWATH.

326 Next, we investigated the differentially expressed proteins using random forest (RF)
 327 analysis (**Fig. 3**). We selected 473 proteins from the S3 SWATH data set after filtering with
 328 Mean Decrease Accuracy > 0. We assessed the 120 min dataset further and found 152 proteins
 329 regulated in both data sets, which separated the malignant from the benign prostate samples in
 330 individual datasets with the area under the curve (AUC) value over 0.95.

331 Another classification algorithm, **XGBoost**, combined with the leave-one-out cross

332 validation, were used to validate the predictability of the 152-protein-signature panel. As
333 shown in **Fig. 3**, we use the 120 min data and 15 min data as training set and validation set
334 respectively. This result further demonstrated the robustness of the S3 SWATH workflow.
335 Throughout the training process, due to the limited number of samples ($n = 68$), we used the
336 leave-one-out cross validation method to judge the effect of the classifier on the training set
337 and adjust the classifier parameters. The trained model then classified the test data set. Using
338 the 120 min data set as the training set and the 15 min data set as the validation set, or vice
339 versa, we observed high AUC using the XGBoost classifier (0.997 and 0.998 respectively).

340 Among the 152 proteins, many well-known diagnostic makers such as AMARCA or drug
341 targets such as IDH, EIF4E [21] have been found. Next we employed ingenuity pathway
342 analysis (IPA) to analyze the pathways represented by the 152 proteins (**Fig. S4-5**) and
343 observed the presence of multiple metabolic pathways such as mitochondrial dysfunction,
344 oxidative phosphorylation, fatty acid oxidation, and the TCA cycle, which is consistent with
345 prior knowledge that metabolism is dysregulated and reprogrammed in prostate cancers [22]
346 (**Fig. S4**). The IPA identified multiple drivers of the dysfunctional protein network observed
347 here, including MYC, TP53 [23], and FOS [24], as well as potential drugs for PCa including
348 decitabine [25], fenofibrate [26], and methotrexate [27] (**Fig. S5**).



349

350 **Figure 3. Identification of differentially expressed proteins between PCa and BPH tissues. (a)**
351 Schematic of the random forest algorithm. The protein matrix generation from 120 min SWATH and S3
352 SWATH involve independent data input and the output results represent the important score (mean
353 decrease accuracy) for each protein. **(b)** A total of 152 overlapping proteins with higher scores were
354 selected to distinguish benign and tumor tissues by AUC in two protein matrices from 120 min SWATH
355 and S3-SWATH. **(c)** A total of 152 proteins were validated by another machinal learning method,
356 XGBoost with leave-one-out cross validation, in two protein matrices.

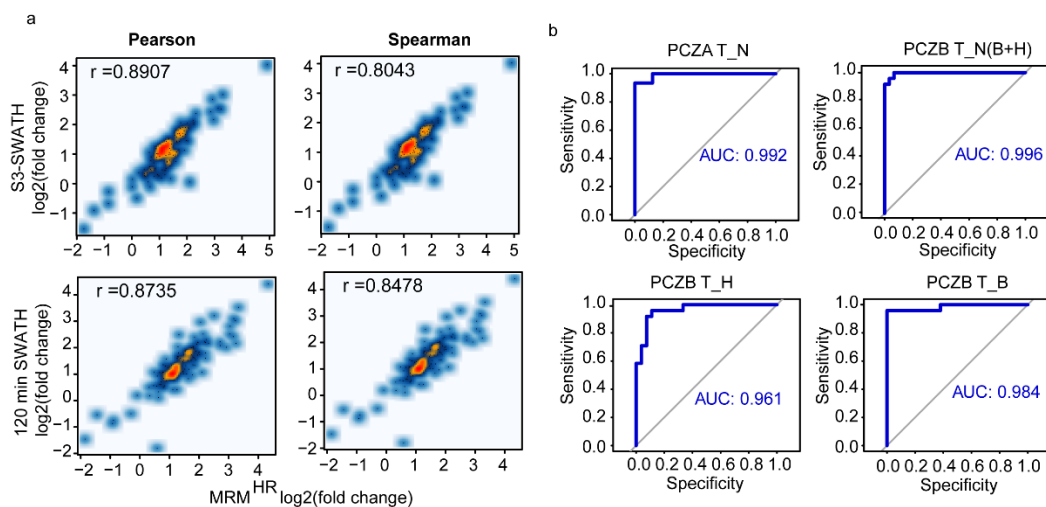
357

358 **Verification of potential diagnostic proteins using MRM^{HR}**

359 We then further validated the S3 SWATH data using a PRM [28] implementation in the
360 TripleTOF® system called MRM^{HR}. The MRM^{HR} method was optimized using a pooled
361 prostate sample to select the best peptides, Q1 isolation windows, and best target fragment
362 ions for quantitation. The protein and peptide information including the RTs were imported
363 into Skyline to build a spectral library. Twelve of the original 152 proteins were rejected due
364 to lower data quality. A total of 261 peptides from 140 proteins and 1429 fragment ions were
365 selected for data extraction. Time scheduling was used to ensure at least eight data points
366 across the LC peaks as well as an optimized accumulation time of 25 ms for each peptide for
367 high quantitative data quality. We also examined the reproducibility of XICs for all peptides
368 in the MRM^{HR} assays. For the five pooled samples measured across five batches, we found

369 that 76.6% of precursors measured from the peptides were quantified with a CV below 20%.
370 The median CV was 13.4% (**Fig. S7a**).

371 To confirm the quantitative accuracy of the S3 SWATH data, we re-analyzed 99
372 samples in the PCZA cohort using the MRM^{HR} method. The protein fold-changes between
373 tumor and normal samples were calculated. We investigated the correlation of 15 min
374 MRM^{HR} and 15 min S3 SWATH quantitative datasets for the 140 proteins based on both
375 Pearson and Spearman correlations. The two datasets were highly correlated with each other,
376 confirming the superior accuracy of both the S3 SWATH and MRM^{HR} approaches (**Fig. 4a**).
377 We further quantified the expression levels of the 140 proteins in an independent prostate
378 cancer cohort, PCZB, containing 30 BPH and 24 PCa in duplicated biological replicates using
379 the same 15 min MRM^{HR} workflow. For the six pooled samples measured across six batches,
380 75.6% of peptide precursors were quantified with a CV below 20%. The median CV is 14.9%
381 (**Fig. S7b**). As shown in **Fig. 4b**, the ROC of the 140-protein-signature panel clearly
382 distinguished PCa from BPH patient groups.

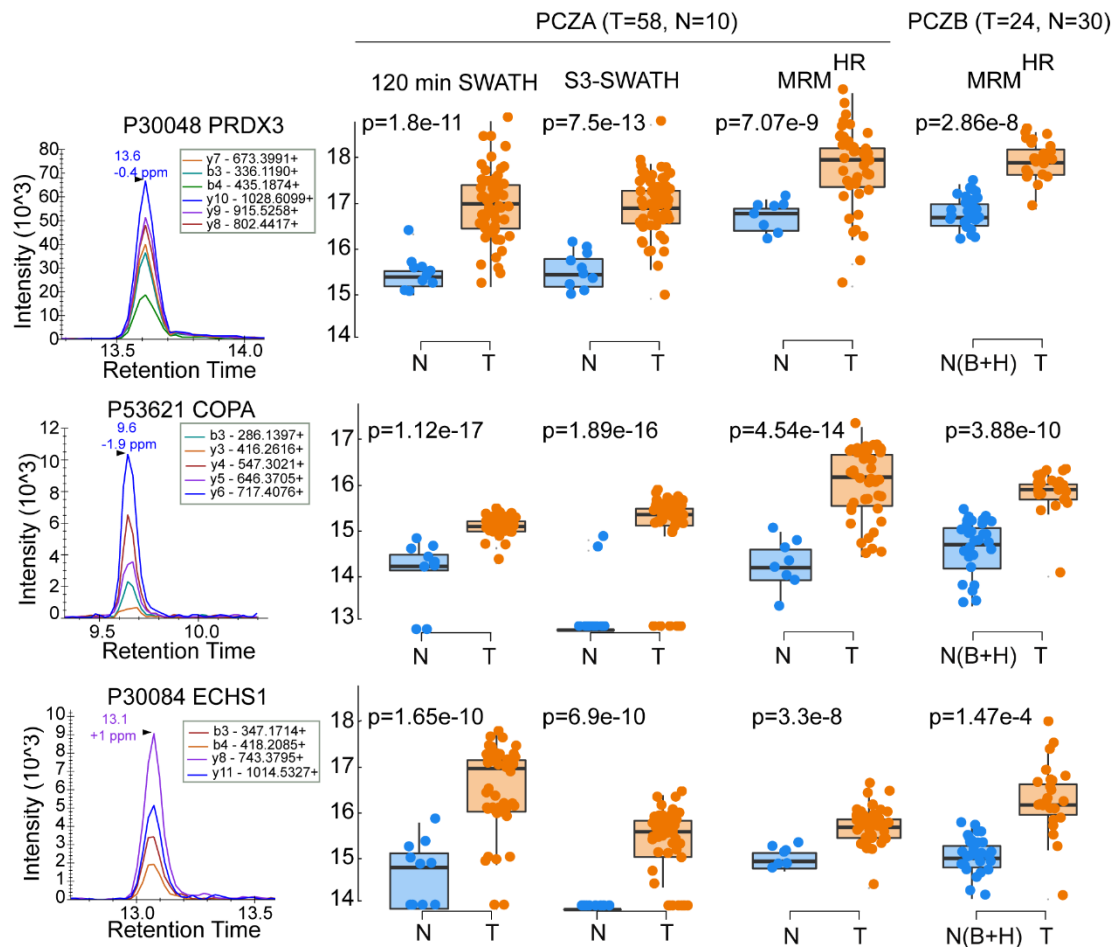


383

384 **Figure 4. Verification of proteomic data using MRM^{HR}.** (a) Pearson and Spearman correlation
385 coefficients between 15 min S3 SWATH and MRM^{HR} datasets were calculated based on the log₂(T/N)
386 of protein expression. (b) The ROC curves of protein quantification from MRM^{HR} to predict the tumor
387 and normal tissues with the random forest algorithm (T: PCa, N: BPH, H: hyperplasia in BPH patients,
388 B: benign in BPH patients).

389

390 We then investigated three proteins—PRDX3 (P30048), COPA (P53621), and ECHS1
391 (P30084)—in detail, prioritized due to their participation in oncogene regulation and potential
392 as drug targets (**Fig. S5**). PRDX3 is an androgen-regulated cell-surface protein which has
393 been reported to be upregulated in PCa as a potential drug target [29, 30]. COPA is a coatmer
394 mediating the biosynthetic protein transport from the endoplasmic reticulum and is associated
395 with cell proliferation [31, 32]. It is overexpressed in PCa tissue and its inhibitor can suppress
396 cell cycle and increase apoptosis of PCa [33]. ECHS1 is an enoyl-CoA hydratase in the
397 mitochondria, which plays important roles in the mitochondrial fatty acid β -oxidation
398 pathway with several reports associating it to HCC and cancers other than PCa [34-36]. Our
399 data show that their expression changes appeared consistent in all three workflows, i.e., 120
400 min SWATH, S3-SWATH, and MRM^{HR} in the PCZA cohort samples (**Fig. 5**). An independent
401 cohort, PCZB, further confirmed their upregulation in prostate tumors (**Fig. 5**). The ROCs of
402 these three proteins from four different datasets distinguishing benign from malignant tissue
403 samples are shown in **Fig. S9**; all of AUC were over than 0.75. The results from the
404 independent cohort PCZB were better than those from cohort PCZA in terms of predictive
405 power, probably due to the higher number of normal samples in the PCZB.



406

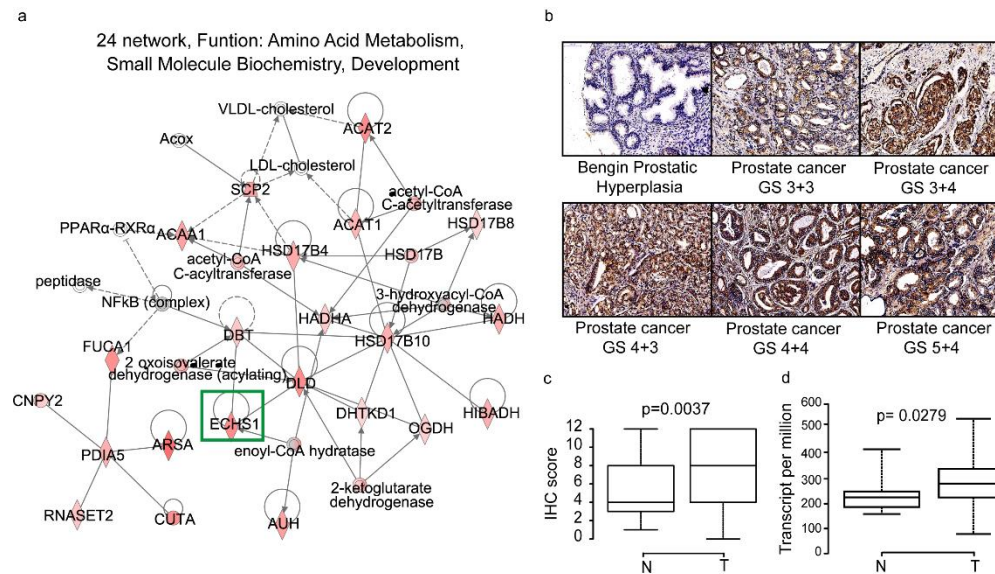
407 **Figure 5. MRM^{HR} validation of potential diagnostic proteins using the PCZA and PCZB.** PRDX3
 408 (peptide: +2 DYGVLLGSLALR), COPA (peptide: +2 DVAVMQLR), ECHS1 (peptide: +2
 409 EGMTAFVEK). The left panel shows the fragment ion extracted-ion chromatograms (XICs) for the
 410 peptide from each protein. The right panel of boxplots shows the peptides quantified in the different
 411 data sets.

412

413 **Verification of protein markers using tissue microarray (TMA)**

414 The most important disordered functions in prostate cancer involve metabolism. We
 415 performed IPA network analysis for the 140 proteins and identified 36 core networks
 416 (Table S4). Among them, Network No. 24, containing ECHS1, is associated with amino acid
 417 metabolism, small molecular biochemistry, and development (Fig. 6a). This network contains
 418 NF- κ B signaling and the molecular associations of lipid metabolism [37], such as the
 419 participation of ACTA2 in the cholesterol biosynthesis pathway, which is involved in
 420 castration-resistant prostate cancer [38, 39]. ACTA2, ARSA, and ECHS1 are involved in fatty
 421 acid β oxidation. ECHS1 was found to be overexpressed in PCa tumors from both PCZA and
 422 PCZB cohorts, in all the four MS datasets in this study. We further applied TMA and
 423 immunohistochemistry staining (IHC) to verify the protein expression changes of ECHS1
 424 measured by MRM^{HR} in the PCZD cohort which contains 30 BPH and 70 PCa (Table 1,
 425 Table S5). Positive cytoplasmic staining of ECHS1 was observed in prostate tumor tissue but
 426 not in BPH tissue (Fig. 6), although the difference among different cancer stages as indicated
 427 by Gleason scores (GS, from 6 to 9) was not significant. We also compared the RNAseq of
 428 normal and tumor in a TCGA dataset containing 549 patients (52 control patients and 497

429 tumor patients) [40]. ECHS1 also show significant different expression (**Fig. 6d**). This data
430 confirms that ECHS1 is a promising prostate cancer biomarker.



431

432 **Figure 6. IHC stain for ECHS1 on tissue microarray.** (a) IPA analysis shows Network No. 24
433 contains ECHS1. (b) TMA shows positive staining of ECHS1 in prostate cancer tissues. The staining
434 images of representative BPH patients (patient SN: 201782041-3) and PCa patients with different
435 Gleason Scores from 6 to 9 are shown (patient SN: GS3+3:201747411-7, GS3+4: 201738874-13,
436 GS4+3: 201742345-10, GS4+4: 201754711-12, GS5+4: 201747749-17). (c) IHC score shows elevated
437 expression of ECHS1 in prostate cancer tissues compared with BPH types. The p value was calculated
438 using a student *t*-test. (d) Transcript copies were calculated from PCa and BPH tissue types based on
439 the TCGA dataset. Student's *t*-test was used to calculate the significance.

440 Conclusion

441 The microflow S3 SWATH enables practical detection of regulated proteins in prostate
442 cancer tissues which are largely identical to those identified by conventional SWATH method
443 and consistent with targeted quantification using MRM^{HR} for shortlisted proteins. Proteins
444 prioritized by the S3 SWATH method were further verified by two independent prostate
445 cancer cohorts. Our multilayer data nominated ECHS1 as a promising biomarker for PCa and
446 potential drug targets. This work presents a novel proteomics pipeline based on an accelerated
447 microflow SWATH MS strategy with potential to accelerate the discovery and verification of
448 protein biomarkers for precision medicine.

449

450 Author Contributions:

451 T.G., C.H., R.S. designed the project. C.H., N.M. and C.C. optimized the S3-SWATH. B.W.,
452 X.Y., X.T., L.C. procured the three prostate cohorts. R.S. performed the PCT-SWATH analysis
453 with help from X.C. C.C. and R.S. performed the MRM^{HR} analysis. W.G., R.S., S.D., J.S.
454 analyzed the data. R.S., Y.Z., C.H. and T.G. wrote the manuscript. C.Y., Z.L assisted data
455 analysis. R.A. gave valuable advice. T.G., Y.Z. supported and supervised the project.

456 **Research Funding:** Zhejiang Provincial Natural Science Foundation of China (Grant No.
457 LR19C050001 to T.G.). Hangzhou Agriculture and Society Advancement Program (Grant No.
458 20190101A04 to T.G.).

459 **Acknowledgments:** The authors thank all collaborators who participated in the procurement
460 of the clinical specimens.

461 **Competing financial interests:** The research group of T.G. is partly supported by SCIEEX,
462 which provides access to prototype instrumentation, and Pressure Biosciences Inc, which
463 provides access to advanced sample preparation instrumentation.

464
465 **Data and materials availability:** The S3 SWATH data are deposited in PRIDE. Project
466 accession: IPX0001645000. The S3 SWATH data are deposited in iProX (IPX0001645001).
467 The MRM^{HR} data are deposited in iProX (IPX0001645002). All the data will be publicly
468 released upon publication.

469

470 References

- 471 1. Loeb, S., et al., *Overdiagnosis and overtreatment of prostate cancer*. Eur Urol, 2014. **65**(6):
472 p. 1046-55.
- 473 2. Bache, N., et al., *A Novel LC System Embeds Analytes in Pre-formed Gradients for Rapid,
474 Ultra-robust Proteomics*. Mol Cell Proteomics, 2018. **17**(11): p. 2284-2296.
- 475 3. Bekker-Jensen, D.B., et al., *An Optimized Shotgun Strategy for the Rapid Generation of
476 Comprehensive Human Proteomes*. Cell Syst, 2017. **4**(6): p. 587-599 e4.
- 477 4. Gillet, L.C., et al., *Targeted data extraction of the MS/MS spectra generated by data-
478 independent acquisition: a new concept for consistent and accurate proteome analysis*.
479 Mol Cell Proteomics, 2012. **11**(6): p. O111 016717.
- 480 5. Rost, H.L., et al., *OpenSWATH enables automated, targeted analysis of data-independent
481 acquisition MS data*. Nat Biotechnol, 2014. **32**(3): p. 219-23.
- 482 6. Guo, T., et al., *Rapid mass spectrometric conversion of tissue biopsy samples into
483 permanent quantitative digital proteome maps*. Nat Med, 2015. **21**(4): p. 407-13.
- 484 7. Zhu, Y., et al., *Identification of Protein Abundance Changes in Hepatocellular Carcinoma
485 Tissues Using PCT-SWATH*. Proteomics Clin Appl, 2019. **13**(1): p. e1700179.
- 486 8. Liu, Y., et al., *Quantitative variability of 342 plasma proteins in a human twin population*.
487 Mol Syst Biol, 2015. **11**(1): p. 786.
- 488 9. Guo, T., et al., *Multi-region proteome analysis quantifies spatial heterogeneity of prostate
489 tissue biomarkers*. Life Sci Alliance, 2018. **1**(2).
- 490 10. Shi, J., et al., *Comparison of protein expression between human livers and the hepatic cell
491 lines HepG2, Hep3B, and Huh7 using SWATH and MRM-HR proteomics: Focusing on
492 drug-metabolizing enzymes*. Drug Metab Pharmacokinet, 2018. **33**(2): p. 133-140.
- 493 11. He, B., et al., *Label-free absolute protein quantification with data-independent acquisition*.
494 J Proteomics, 2019. **200**: p. 51-59.
- 495 12. Colgrave, M.L., et al., *Comparing Multiple Reaction Monitoring and Sequential Window
496 Acquisition of All Theoretical Mass Spectra for the Relative Quantification of Barley Gluten
497 in Selectively Bred Barley Lines*. Anal Chem, 2016. **88**(18): p. 9127-35.
- 498 13. Le Duff, M., et al., *Regulation of senescence escape by the cdk4-EZH2-AP2M1 pathway
499 in response to chemotherapy*. Cell Death Dis, 2018. **9**(2): p. 199.
- 500 14. Vowinckel, J., et al., *Cost-effective generation of precise label-free quantitative proteomes
501 in high-throughput by microLC and data-independent acquisition*. Sci Rep, 2018. **8**(1): p.
502 4346.
- 503 15. Liu, Y., et al., *Multi-omic measurements of heterogeneity in HeLa cells across laboratories*.
504 Nat Biotechnol, 2019. **37**(3): p. 314-322.
- 505 16. Yi Zhu 1, 3*, Tobias Weiss 4*, Qiushi Zhang 1,2, Rui Sun 1,2, Bo Wang 5, Zhicheng Wu 1,2,

- 506 Qing Zhong 6,7, Xiao Yi 1,2 , Huanhuan Gao 1,2, Xue Cai 1,2, Guan Ruan 1,2, Tiansheng
507 Zhu 1,2, Chao Xu, Sai Lou 9, Xiaoyan Yu 10, Ludovic Gillet 3, Peter Blattmann 3, Karim
508 Saba 11, Christian D.Fankhauser 11, Michael B. Schmid 11, Dorothea Rutishauser 6, Jelena
509 Ljubicic 6, Ailsa, Christiansen 6, Christine Fritz 6, Niels J. Rupp 6, Cedric Poyet 11, Elisabeth
510 Rushing 12, Michael Weller 4, Patrick Roth 4, Eugenia Haralambieva 6, Silvia Hofer 13,
511 Chen Chen 14, Wolfram Jochum 15, Xiaofei Gao 1,2, Xiaodong Teng 5, Lirong Chen 10,
512 Peter J. Wild 6,16#, Ruedi Aebersold 3,17# , Tiannan Guo, *High-throughput proteomic
513 analysis of FFPE tissue samples facilitates tumor stratification*. biorxiv, 2019.
- 514 17. Zhu, Y. and T. Guo, *High-Throughput Proteomic Analysis of Fresh-Frozen Biopsy Tissue
515 Samples Using Pressure Cycling Technology Coupled with SWATH Mass Spectrometry*.
516 *Methods Mol Biol*, 2018. **1788**: p. 279-287.
- 517 18. MacLean, B., et al., *Skyline: an open source document editor for creating and analyzing
518 targeted proteomics experiments*. *Bioinformatics*, 2010. **26**(7): p. 966-8.
- 519 19. Rosenberger, G., et al., *A repository of assays to quantify 10,000 human proteins by
520 SWATH-MS*. *Sci Data*, 2014. **1**: p. 140031.
- 521 20. Guo T1, Li L3, Zhong Q4,5, Rupp NJ4, Charmpi K3, Wong CE4, Wagner U4, Rueschoff JH4,
522 Jochum W6, Fankhauser CD7, Saba K7, Poyet C7, Wild PJ4,8, Aebersold R1,9, Beyer A,
523 *Multi-region proteome analysis quantifies spatial heterogeneity of prostate tissue
524 biomarkers*. *Life Sci Alliance.*, 2018.
- 525 21. Counihan, J.L., E.A. Grossman, and D.K. Nomura, *Cancer Metabolism: Current
526 Understanding and Therapies*. *Chem Rev*, 2018. **118**(14): p. 6893-6923.
- 527 22. Wu, X., et al., *Lipid metabolism in prostate cancer*. *Am J Clin Exp Urol*, 2014. **2**(2): p. 111-
528 20.
- 529 23. Thompson, T.C., et al., *Loss of p53 function leads to metastasis in ras+myc-initiated
530 mouse prostate cancer*. *Oncogene*, 1995. **10**(5): p. 869-79.
- 531 24. Edwards, J., et al., *The role of c-Jun and c-Fos expression in androgen-independent
532 prostate cancer*. *J Pathol*, 2004. **204**(2): p. 153-8.
- 533 25. Momparler, R.L., *Epigenetic therapy of cancer with 5-aza-2'-deoxycytidine (decitabine)*.
534 *Semin Oncol*, 2005. **32**(5): p. 443-51.
- 535 26. Panigrahy, D., et al., *PPARalpha agonist fenofibrate suppresses tumor growth through
536 direct and indirect angiogenesis inhibition*. *Proc Natl Acad Sci U S A*, 2008. **105**(3): p. 985-
537 90.
- 538 27. Saxman, S., et al., *Phase III trial of cyclophosphamide versus cyclophosphamide,
539 doxorubicin, and methotrexate in hormone-refractory prostatic cancer. A Hoosier
540 Oncology Group study*. *Cancer*, 1992. **70**(10): p. 2488-92.
- 541 28. Peterson, A.C., et al., *Parallel reaction monitoring for high resolution and high mass
542 accuracy quantitative, targeted proteomics*. *Mol Cell Proteomics*, 2012. **11**(11): p. 1475-
543 88.
- 544 29. Lin, J.F., et al., *Identification of candidate prostate cancer biomarkers in prostate needle
545 biopsy specimens using proteomic analysis*. *Int J Cancer*, 2007. **121**(12): p. 2596-605.
- 546 30. Whitaker, H.C., et al., *Peroxiredoxin-3 is overexpressed in prostate cancer and promotes
547 cancer cell survival by protecting cells from oxidative stress*. *Br J Cancer*, 2013. **109**(4): p.
548 983-93.
- 549 31. Harter, C., et al., *Nonclathrin coat protein gamma, a subunit of coatomer, binds to the*

- 550 *cytoplasmic dilysine motif of membrane proteins of the early secretory pathway*. Proc Natl
551 Acad Sci U S A, 1996. **93**(5): p. 1902-6.
- 552 32. Gerich, B., et al., *Non-clathrin-coat protein alpha is a conserved subunit of coatamer and*
553 *in Saccharomyces cerevisiae is essential for growth*. Proc Natl Acad Sci U S A, 1995. **92**(8):
554 p. 3229-33.
- 555 33. Iglesias-Gato, D., et al., *The Proteome of Primary Prostate Cancer*. Eur Urol, 2016. **69**(5):
556 p. 942-52.
- 557 34. Zhang, Y.K., et al., *Enoyl-CoA hydratase-1 regulates mTOR signaling and apoptosis by*
558 *sensing nutrients*. Nat Commun, 2017. **8**(1): p. 464.
- 559 35. Sharpe, A.J. and M. McKenzie, *Mitochondrial Fatty Acid Oxidation Disorders Associated*
560 *with Short-Chain Enoyl-CoA Hydratase (ECHS1) Deficiency*. Cells, 2018. **7**(6).
- 561 36. Chang, Y., et al., *ECHS1 interacts with STAT3 and negatively regulates STAT3 signaling*.
562 FEBS Lett, 2013. **587**(6): p. 607-13.
- 563 37. De Nunzio, C., et al., *The correlation between metabolic syndrome and prostatic diseases*.
564 Eur Urol, 2012. **61**(3): p. 560-70.
- 565 38. Ylitalo, E.B., et al., *Subgroups of Castration-resistant Prostate Cancer Bone Metastases*
566 *Defined Through an Inverse Relationship Between Androgen Receptor Activity and*
567 *Immune Response*. Eur Urol, 2017. **71**(5): p. 776-787.
- 568 39. Twiddy, A.L., C.G. Leon, and K.M. Wasan, *Cholesterol as a potential target for castration-*
569 *resistant prostate cancer*. Pharm Res, 2011. **28**(3): p. 423-37.
- 570 40. Chandrashekar, D.S., et al., *UALCAN: A Portal for Facilitating Tumor Subgroup Gene*
571 *Expression and Survival Analyses*. Neoplasia, 2017. **19**(8): p. 649-658.

572